AD-A067 284 NAVAL UNDERWATER SYSTEMS CENTER NEW LONDON CONN NEW --ETC F/G 12/1
A STATE VARIABLE APPROACH TO STATIONARY TIME SERIES WITH APPLIC--ETC(U)
FEB 79 R J NIELSEN

UNCLASSIFIED NUSC-TR-5893 NL

1 OF 1
AD A067 284

END
DATE FILMED
6 -79
DDC

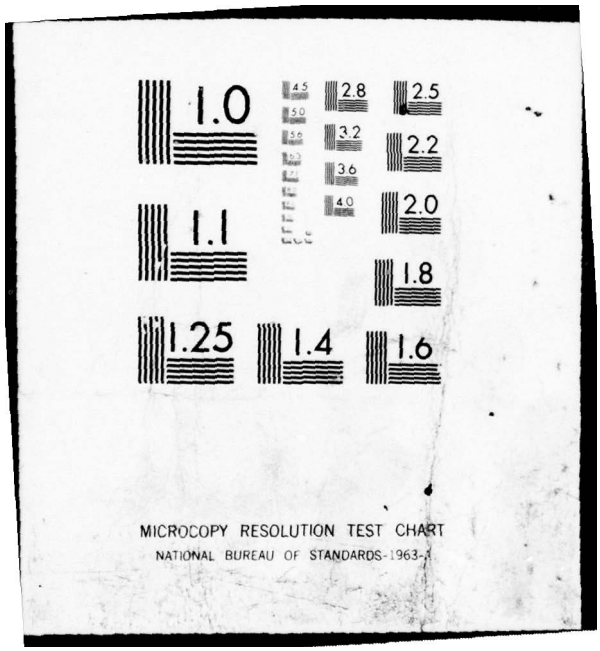
1.0
1.1
1.25
1.4
1.6
1.8
2.0
2.2
2.5
2.8
3.2
3.6
4.0
4.5
5.0
5.6
MICROCOPY RESOLUTION TEST CHART
NATIONAL BUREAU OF STANDARDS-1963-A

NUSC Technical Report 5893

12

LEVEL II

A State Variable Approach to Stationary Time Series With Application for Predicting Displacement In a Large Underwater Suspended Array

Richard J. Nielsen
Special Projects Department

21 February 1979

NUSC

NAVAL UNDERWATER SYSTEMS CENTER
Newport, Rhode Island • New London, Connecticut

(14) NUSC-TR-5893

REPORT DOCUMENTATION PAGE

READ INSTRUCTIONS BEFORE COMPLETING FORM

1. REPORT NUMBER: TR 5893
2. GOVT ACCESSION NO.
3. RECIPIENT'S CATALOG NUMBER

(6) 4. TITLE (and Subtitle): A STATE VARIABLE APPROACH TO STATIONARY TIME SERIES WITH APPLICATION FOR PREDICTING DISPLACEMENT IN A LARGE UNDERWATER SUSPENDED ARRAY.

5. TYPE OF REPORT & PERIOD COVERED

6. PERFORMING ORG. REPORT NUMBER

(10) 7. AUTHOR(s): Richard J. Nielsen

8. CONTRACT OR GRANT NUMBER(s)

(9) Technical rept.,

9. PERFORMING ORGANIZATION NAME AND ADDRESS
Naval Underwater Systems Center
New London Laboratory
New London, CT 06320

10. PROGRAM ELEMENT, PROJECT, TASK AREA & WORK UNIT NUMBERS
631Y00

11. CONTROLLING OFFICE NAME AND ADDRESS
Naval Underwater Systems Center
Newport, RI 02840

(11) 12. REPORT DATE: 21 Feb 1979

13. NUMBER OF PAGES: 45

14. MONITORING AGENCY NAME & ADDRESS (if different from Controlling Office)

(12) 49p.

15. SECURITY CLASS. (of this report): Unclassified

15a. DECLASSIFICATION/DOWNGRADING SCHEDULE

16. DISTRIBUTION STATEMENT (of this Report)

Approved for public release; distribution unlimited.

17. DISTRIBUTION STATEMENT (of the abstract entered in Block 20, if different from Report)

18. SUPPLEMENTARY NOTES

19. KEY WORDS (Continue on reverse side if necessary and identify by block number)

Array Displacement
Kalman Filter
State Space Equation
State Variable Representation
Stationary Systems
Stationary Time Series
Underwater Suspended Arrays
Wiener Filter

20. ABSTRACT (Continue on reverse side if necessary and identify by block number)

State variable representation of systems is developed, together with the solution to the state space equation. The Kalman filter theory is outlined along with its extension to stationary processes and prediction. The relationship of the Kalman filter to the Wiener filter is also indicated.

The motion of a large underwater suspended array is described in terms of the power spectrum of its displacement fluctuations. The variance of the error in the predicted array displacement is estimated, using Kalman filter theory

DD FORM 1 JAN 73 1473

405 918

20. Cont'd

based on 1- and 2-pole approximations of the displacement power spectrum. Closed-form expressions are maintained throughout the development. The results of the study show that the predicted array displacements are sensitive to the power spectral approximation, and that large errors in the displacement predictions can occur in relatively short periods of time.

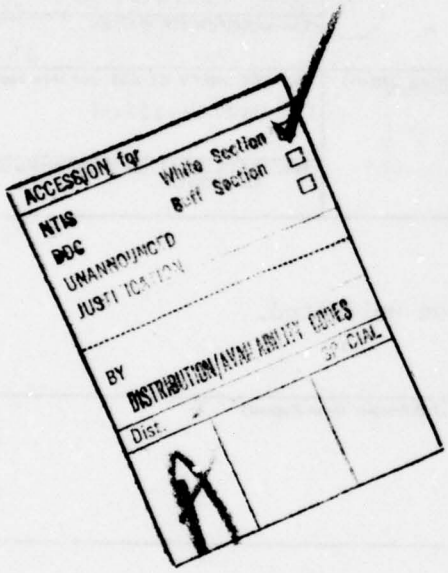

TABLE OF CONTENTS

LIST OF ILLUSTRATIONS

LIST OF SYMBOLS

MATRICES

$F(t)$	Coefficient matrix
$G(t)$	Coefficient matrix
$H(t)$	Coefficient matrix
$R(s)$	Spectral density
$\Psi_{\underline{w}}(t)$	Plant noise covariance
$\Psi_{\underline{v}}(t)$	Measurement noise covariance
$K(t)$	Kalman gain
$A(t)$	Coefficient matrix
$\Phi(t,\tau)$	Transition matrix
$V_e(t)$	Error variance matrix
I	Identity matrix
$A(t,\tau)$	Weighting matrix
$R(\tau)$	Correlation function
$W_o(s)$	Optimum Wiener filter
$\Delta(s)$	Spectral factored matrix

VECTORS

$\underline{x}(t)$	State vector
$\underline{w}(t)$	Plant noise
$\underline{v}(t)$	Measurement noise
$\underline{z}(t)$	Observation vector
$\underline{y}(t)$	Signal

SCALARS

a_i	Coefficients

LIST OF SYMBOLS (Cont'd)

b_i	Coefficients
β_i	Coefficients
ϵ	Standard error
τ	Function length
Δf	Equivalent bandwidth
σ_z^2	Data variance
$X(k)$	Spectral estimate
P	Power (ft^2/Hz)
ω	Radian frequency
f	Frequency
λ_i	Eigenvalues
α_i	Coefficients
n	Number of poles in either half-plane
L	Sample length
Δt	Sampling interval
N	Total samples
m	Number of lag values

MISCELLANEOUS

det	Determinant
cov	Covariance
E	Expectation
δ	Delta function
s	Laplace operator
$\hat{}$	Estimated quantities (e.g., $\hat{x}$)
.	Derivative (e.g., $\dot{x}$)

LIST OF SYMBOLS (Cont'd)

$(t\|t_1)$	Function at t based on measurements at t_1
PR	Physically realizable
_	Vector (e.g., $\underline{x}$)
μ	Mean
var	Variance
$\mathcal{F}$	Fourier transform

A STATE VARIABLE APPROACH TO STATIONARY TIME SERIES WITH APPLICATION FOR PREDICTING DISPLACEMENT IN A LARGE UNDERWATER SUSPENDED ARRAY

INTRODUCTION

The original extensive treatment of stationary time series analysis was developed by Wiener (1949) in his classical work "Extrapolation, Interpolation and Smoothing of Stationary Time Series," reference 1. Wiener's results were expressed in the frequency domain and could not readily be extended to nonstationary problems. In 1960 Kalman, reference 2, extended Wiener's work to nonstationary time domain problems. Although the real power of the Kalman filter theory lies in its ability to handle the nonstationary case, computational advantages of the Kalman filter make it worth considering for many stationary problems.

The background information necessary to understand the Kalman filter computational techniques has been included in this report. In most cases, equations are stated without proof, since lengthy derivations are usually required for their development. Several texts (references 3, 4, and 5), which treat this subject with much more rigor and detail, are available. However, most of the development and notation used here is consistent with that used by Sage and Melsa, reference 4.

As an example of the application of Kalman filter theory to prediction, the displacement fluctuations of a large underwater suspended array are investigated. Both the 1- and 2-pole prediction estimates along with the associated error variance, are determined.

Prediction of the array displacement is motivated by a desire both to reduce the corruptive effects of sampling the array position and to decrease the number of active transmissions in the vicinity of the array.

BACKGROUND

Some of the notations used in this report may not be familiar to all the individuals interested in this subject. Therefore, this section has been included as an aid to understanding the material that is to follow. The information is admittedly brief, and those desiring more detail should refer to Sage and Melsa, reference 4.

STATE VARIABLE NOTATION

Linear systems can be represented in a vector form known as the state vector differential equation,

$$\dot{\underline{x}}(t) = F(t)\ \underline{x}(t) + G(t)\ \underline{w}(t),$$

where the state vector $\underline{x}(t)$ is related to the system dependent variable and its derivatives.

The solution of the state equation is given by

$$\underline{x}(t) = \Phi(t,\ t_o)\ \underline{x}(t_o) + \int_{t_o}^{t} \Phi(t,\ \tau)\ G(\tau)\ \underline{w}(\tau)\ d\tau,$$

where $\Phi(t,t_o)$ (called the state transition matrix) is given by the solution of

$$\frac{d}{dt}\ [\Phi(t,\ t_o)] \ = \ \dot{\Phi}(t,\ t_o) = F(t)\ \Phi(t,\ t_o),$$

with the initial condition $\Phi(t_o,\ t_o) = I$.

If, in addition, F(t) is time invariant, the state transition matrix is given by

$$\Phi(t,\ t_o) = e^{F\ (t-t_o)} = \alpha_o I + \alpha_1 F + \ldots + \alpha_{n-1}\ F^{n-1};$$

when the eigenvalues of F are distinct, the α_i are given by solving the following sets of equations:

$$\alpha_0 + \alpha_1\lambda_1 + \ldots + \alpha_{n-1}\ \lambda_1^{n-1} = e^{\lambda_1(t-t_o)}$$

$$\alpha_0 + \alpha_1\lambda_2 + \ldots + \alpha_{n-1}\ \lambda_2^{n-1} = e^{\lambda_2(t-t_o)}$$

$$\vdots \quad \vdots \qquad\qquad \vdots \qquad\qquad \vdots$$

$$\alpha_0 + \alpha_1\ \lambda_n + \ldots + \alpha_{n-1}\ \lambda_n^{n-1} = e^{\lambda_n(t-t_o)}.$$

KALMAN FILTER THEORY

Suppose we have a system whose behavior can be described by the state equation

$$\dot{\underline{x}}(t) = F(t)\ \underline{x}\ (t)\ G(t)\ \underline{w}(t) \qquad \text{(message model)},$$

where $\underline{w}(t)$ is a zero-mean white noise process with covariance

$$\text{cov}\ \{\underline{w}(t),\ \underline{w}(\tau)\} = V_{\underline{w}}(t,\ \tau) = \Psi_{\underline{w}}(t)\ \delta(t-\tau)$$

and the initial mean and variance of the state $\underline{x}(t)$ is known

$$\mu_{\underline{x}}(o) = E\ \{\underline{x}\ (o)\} \qquad V_{\underline{x}}(o) = \text{var}\ \{\underline{x}(o)\}.$$

Further suppose that some measurements are made which are related to the state $\underline{x}\ (t)$ as

$$\underline{z}(t) = H(t)\ \underline{x}(t) + \underline{v}(t) \qquad \text{(observation model)},$$

where $\underline{v}(t)$ is zero-mean white noise with

$$\text{cov}\ \{\underline{v}(t),\ \underline{v}(\tau)\} = V_{\underline{v}}(t,\ \tau) = \Psi_{\underline{v}}(t)\ \delta(t-\tau)$$

and $\underline{w}$ and $\underline{v}$ are uncorrelated:

$$\text{cov}\ \{\underline{w}\ (t),\ \underline{v}\ (\tau)\} = V_{\underline{w}\ \underline{v}}(t,\ \tau) = 0.$$

Based on the foregoing model, the Kalman filter desires to make an estimate of the state $\underline{x}(t)$. In addition, the estimator must meet the following requirements:

(1) The form of the estimator is linear,

$$\hat{\underline{x}}(t) = \underline{a}_o(t) + \int_o^t A(t,\ \tau)\ \underline{z}(\tau)\ d\tau$$

(2) The bias error of the estimator is zero,

$$E\ \{\underline{x}(t) - \hat{\underline{x}}(t)\} = E\ \{\underline{x}_e(t)\} = 0.$$

(3) The trace of the variance of the error is a minimum,

$$\text{tr}\ [\text{var}\ \{\underline{x}(t) - \hat{\underline{x}}(t)\}] \qquad \text{minimum}.$$

The estimator which can be developed to meet the foregoing requirements is the "optimum linear minimum-error-variance sequential state estimator," or more commonly, the "Kalman filter." A complete summary of the Kalman filter algorithm is shown in table 1 and diagrammed in figure 1.

STATIONARY PROCESSES

Many problems can be considered stationary or almost stationary. This fact, together with the knowledge that the Kalman filter has many computational advantages over the Wiener filter, makes it worth considering the Kalman filter for the solution of stationary problems.

Table 1. Continuous Kalman Filter Algorithm

Models	Algorithms
Message	Filter
$\dot{\underline{x}}(t) = F(t)\,\underline{x}(t) + G(t)\,\underline{w}(t)$	$\dot{\hat{\underline{x}}}(t) = F(t)\,\hat{\underline{x}}(t) + K(t)\left[\underline{z}(t) - H(t)\,\hat{\underline{x}}(t)\right]$
Observation	Gain
$\underline{z}(t) = H(t)\,\underline{x}(t) + \underline{v}(t)$	$K(t) = V_{e_{\underline{x}}}(t)\,H^T(t)\,\Psi_{\underline{v}}^{-1}(t)$
	Error Variance
	$\dot{V}_{e_{\underline{x}}}(t) = F(t)\,V_{e_{\underline{x}}}(t) + V_{e_{\underline{x}}}(t)\,F^T(t) - V_{e_{\underline{x}}}(t)\,H^T(t)\,\Psi_{\underline{v}}^{-1}(t)\,H(t)\,V_{e_{\underline{x}}}(t) + G(t)\,\Psi_{\underline{w}}(t)\,G^T(t)$

Prior Statistics

$E\{\underline{w}(t)\} = E\{\underline{v}(t)\} = \underline{0} \qquad E\{\underline{x}(0)\} = \mu_{\underline{x}}(0)$

$\operatorname{cov}\{\underline{w}(t), \underline{w}(\tau)\} = \Psi_{\underline{w}}(t)\,\delta(t-\tau)$

$\operatorname{cov}\{\underline{w}(t), \underline{v}(\tau)\} = \operatorname{cov}\{\underline{x}(0), \underline{w}(t)\} = \operatorname{cov}\{\underline{x}(0), \underline{v}(t)\} = 0$

$\operatorname{var}\{\underline{x}(0)\} = V_{\underline{x}}(0)$

$\operatorname{cov}\{\underline{v}(t), \underline{v}(\tau)\} = \Psi_{\underline{v}}(t)\,\delta(t-\tau)$

Initial Conditions

$\hat{\underline{x}}(0) = E\{\underline{x}(0)\} = \mu_{\underline{x}}(0)$

$V_{e_{\underline{x}}}(0) = \operatorname{var}\{\underline{x}(0)\} = V_{\underline{x}}(0)$

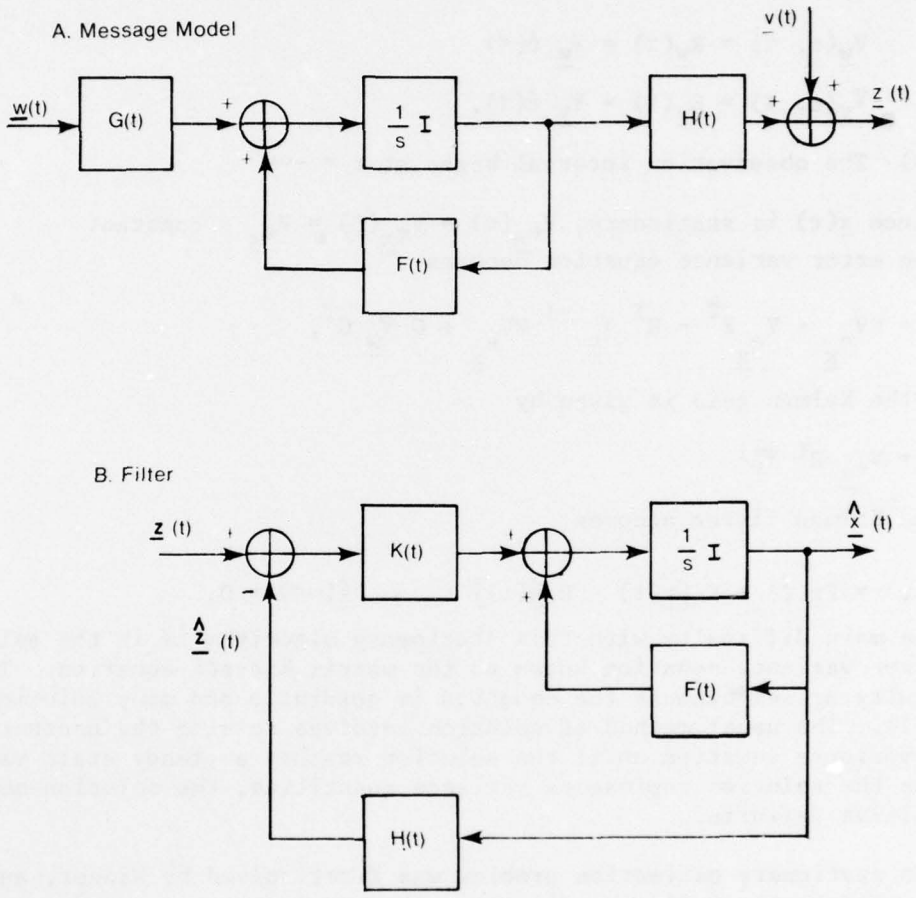

Figure 1. Kalman Filter

For the stationary case, the following assumptions must be satisfied:

(1) The message and observation models are time invariant,

$$\dot{\underline{x}}(t) = F\underline{x}(t) + G\,\underline{w}(t)$$
$$\underline{z}(t) = H\underline{x}(t) + \underline{v}(t).$$

(2) The input and measurement noise are at least wide sense stationary,

$$V_{\underline{w}}(t,\ \tau) = R_{\underline{w}}(\tau) = \Psi_{\underline{w}}\ \delta(\tau)$$
$$V_{\underline{v}}(t,\ \tau) = R_{\underline{v}}(\tau) = \Psi_{\underline{v}}\ \delta(\tau).$$

(3) The observation interval began at $t = -\infty$.

Since $\underline{x}(t)$ is stationary, $V_{e_{\underline{x}}}(t) = V_{e_{\underline{x}}}(0) = V_{e_{\underline{x}}} = \text{constant}$ and the error variance equation becomes

$$0 = FV_{e_{\underline{x}}} + V_{e_{\underline{x}}}F^T - H^T \Psi_{\underline{v}}^{-1} HV_{e_{\underline{x}}} + G\,\Psi_{\underline{w}}\,G^T,$$

where the Kalman gain is given by

$$K = V_{e_{\underline{x}}}\,H^T\,\Psi_{\underline{v}}^{-1}$$

and the Kalman filter becomes

$$\dot{\hat{\underline{x}}}(t) = F\hat{\underline{x}}(t) + K\left[\underline{z}(t) - H\,\hat{\underline{x}}(t)\right] \qquad \hat{\underline{x}}(-\infty) = \underline{0}.$$

The main difficulty with this stationary algorithm is in the solution of the error variance equation known as the matrix Riccati equation. This difficulty arises because the equation is quadratic and many solutions are possible. The usual method of solution involves solving the nonstationary error variance equation until the solution reaches a steady state value. Because the solution represents variance quantities, the solution must also be positive definite.

The stationary estimation problem was first solved by Wiener, and is represented by the following diagram.

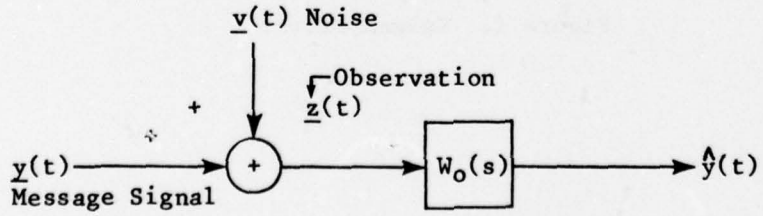

Wiener showed that the optimum linear minimum error variance filter $W_o(s)$, when $\underline{y}(t)$ and $\underline{v}(t)$ are uncorrelated, is given by

$$W_o(s) = \left[R_{\underline{y}}(s)\ \Delta^{-T}(s)\right]_{PR}\ \Delta^{-1}(s),$$

where

PR corresponds to physically realizable,

$R_{\underline{y}}(s)$ = message spectral density = $\mathfrak{F}\left\{R_{\underline{y}}(\tau)\right\} = \mathfrak{F}\left\{V_{\underline{y}}(t+\tau, t)\right\}$, and $\Delta(s)$ is given by

$$R_{\underline{z}}(s) = R_{\underline{y}}(s) + R_{\underline{v}}(s) = \Delta(s)\,\Delta^{T}(-s).$$

The matrix $\Delta(s)$ is such that the rational function det $[\Delta(s)]$ has all its poles and zeros in the left half of the s-plane.

The equivalence of the Kalman and Wiener filters can be shown by letting

$$\underline{y}(t) = H\,\underline{x}(t).$$

In this case, it can be shown that the message spectral density becomes

$$R_{\underline{y}}(s) = H(SI-F)^{-1}\,G\Psi_{\underline{w}}\,G(-SI-F^{T})^{-1}H^{T},$$

and the optimum Wiener filter is given by

$$W_{o}(s) = H(SI-F+KH)^{-1}K.$$

For the particular case of scalar observations, the spectral factorization becomes

$$R_{y}(S) = \left[R_{y}(s)\right]^{+} \quad \left[R_{y}(s)\right]^{-},$$

where the + and - represent left-half and right-half plane poles and zeros, respectively.

In particular, if we write the spectrum as a function of rational polynomials

$$\left[R_{y}(s)\right]^{+} = \frac{\alpha_{o} + \alpha_{1}\,S + \ldots + \alpha_{m}\,S^{m}}{\beta_{o} + \beta_{1}\,S + \ldots + S^{n}} \qquad m < n,$$

then the coefficient matrices in the Kalman model become

$$F = \begin{bmatrix} 0 & 1 & 0 & \cdots & 0 \\ 0 & 0 & 1 & \cdots & 0 \\ \cdot & \cdot & \cdot & \cdots & \cdot \\ \cdot & \cdot & \cdot & \cdots & \cdot \\ \cdot & \cdot & \cdot & \cdots & \cdot \\ 0 & 0 & \cdot & \cdots & 0 \\ 0 & 0 & \cdot & \cdots & 1 \\ \beta_{o} & -\beta_{1} & \cdot & \cdots & -\beta_{n-1} \end{bmatrix} \qquad H^{T} = \begin{bmatrix} \alpha_{0} \\ \alpha_{1} \\ \cdot \\ \cdot \\ \cdot \\ \alpha_{m} \\ 0 \\ 0 \end{bmatrix}$$

$$\Psi_{\underline{w}} = \begin{bmatrix} 0 & 0 & . & . & . & 0 \\ 0 & 0 & . & . & . & 0 \\ . & . & & & & . \\ . & . & & & & . \\ . & . & & & & . \\ 0 & 0 & . & . & 0 & 0 \\ 0 & 0 & . & . & 0 & 1 \end{bmatrix} \qquad G = I \ .$$

EXTENSION TO PREDICTION

Based on measurements to time t_1, there are three classes of state estimation. Consider the following diagram, depicting one component of the state vector $\underline{x}(t)$.

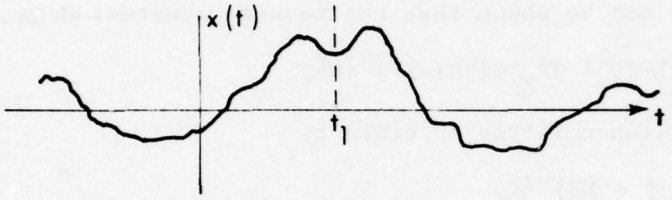

If we define $\hat{\underline{x}}(t \mid t_1) = E\{\underline{x}(t) \mid \underline{z}(t_1)\}$,
the classifications are:

(1) Filtering ($t = t_1$),

$$\hat{\underline{x}}(t \mid t_1) = \hat{\underline{x}}(t_1 \mid t_1) = \hat{\underline{x}}(t_1),$$

(2) Smoothing ($t < t_1$),

(3) Predicting ($t > t_1$).

The Kalman filter, which estimates the current state, has been covered in the previous section. The smoothing problem is of interest when improved estimates are required for previous values based on the collection of more data. The prediction problem arises when some future value must be estimated from present measurements.

The smoothing problem would amount to a fairly large extension of this material and will not be covered here. The prediction problem, however, amounts to a simple extension of the Kalman filter and a treatment of this problem follows.

The state at time t is given by

$$\underline{x}(t) = \Phi(t, t_1)\, \underline{x}(t_1) + \int_{t_1}^{t} \Phi(t, \tau)\, G(\tau)\, \underline{w}(\tau)\, d\tau.$$

Taking the conditional mean of both sides, we obtain

$$\underline{\hat{x}}(t \mid t_1) = E\left\{\underline{x}(t) \mid \underline{z}(t_1)\right\} = \Phi(t, t_1)\,\underline{\hat{x}}(t_1)$$

$$+ \int_{t_1}^{t} \Phi(t, \tau)\, G(\tau)\, E\left\{\underline{w}(\tau) \mid \underline{z}(t_1)\right\} d\tau .$$

Since $\underline{w}(\tau)$ is a white noise process,

$$E\left\{\underline{w}(\tau) \mid \underline{z}(t_1)\right\} = E\left\{\underline{w}(\tau)\right\} = 0 \qquad \text{for } \tau \geq t_1,$$

the predictor equation becomes

$$\underline{\hat{x}}(t \mid t_1) = \Phi(t, t_1)\,\underline{\hat{x}}(t_1) \qquad \text{for } t \geq t_1.$$

Other forms of the predictor equation can be obtained, depending on how t varies with respect to t_1. However, all forms are the same for stationary processes.

The prediction error is given by

$$\underline{x}_e(t \mid t_1) = \underline{x}(t) - \underline{\hat{x}}(t \mid t_1),$$

and the variance of the prediction error is

$$V_{\underline{x}_e}(t \mid t_1) = \operatorname{var}\left\{\underline{x}_e(t \mid t_1)\right\},$$

$$V_{\underline{x}_e}(t \mid t_1) = \Phi(t, t_1)\, V_{\underline{x}_e}(t_1)\, \Phi^T(t, t_1)$$

$$+ \int_{t_1}^{t} \Phi(t, \tau)\, G(\tau)\, \Psi_{\underline{w}}(\tau)\, G^T(\tau)\, \Phi^T(t, \tau)\, d\tau .$$

The Kalman filter can be extended to handle other classes of problems. For instance, the problem of nonwhite noise can be handled by augmenting the state vector with additional states. Also, the Kalman filter can be used in the solution of nonlinear estimation problems, provided that certain justifiable assumptions can be made. These extensions of the Kalman filter will not be covered here, since they are not applicable to the problems under consideration.

EXPERIMENT

The preceding sections have still not made it clear as to how the Kalman filter techniques can be applied to a practical problem. The author thought that the best way to demonstrate these techniques would be through the use of an example. The example selected arose from some measurements made on a large underwater suspended array, reference 6. The end result of the signal

processing will be an estimate of the variance of the error associated with predicting future array displacements based on current measured displacements.

DATA ACQUISITION

Three transponder assemblies, figure 2, were installed by the ALCOA R/V SEA PROBE on the horizontal portion of the underwater suspended array. Other transponders were installed on the ocean bottom both inline and normal to the array. A diagram of the resulting experimental configuration is shown in figure 3.

The procedure for data collection was to interrogate an array transponder (P1) with a shipboard transponder (P0). The array transponder would, in turn, interrogate the bottom transponders (P7 and P8), which would reactivate the array transponder. From the sequence of arrivals received onboard the ship, it was possible to determine the slant range between array and bottom transponders. The slant range could, in turn, be converted to Cartesian coordinates.

The array, having a large mass, was assumed not to move during the sampling sequence, which lasted approximately 10 seconds. Further, the travel time variability due to ship drift was found to be predictable, and thus could be removed from the computations. The array position was sampled once each minute, which was more than sufficient to prevent aliasing.

DATA PROCESSING

A sample of the raw data is shown in figure 4. The different symbols represent data collected from different transponder units. In order that a complete data set could be obtained, the raw data were smoothed to eliminate bad data points and to fill in missing data points. The smoothed data were then sampled at 6 minute intervals to form the time series from which further processing would be accomplished.

A time series plot of the resulting smoothed data is shown in figure 5. The length of the sample is 262 hours, and both the relative displacement fluctuations inline with (Δx) and orthogonal to (Δy) the array are shown. The significant low frequency periods appearing in the time series are motions due to inertial effects of ocean currents in the vicinity of the array. This is perhaps better illustrated through the use of the autocorrelation function, figure 6, where the principal period of the displacement fluctuations is 22.5 hours. This period corresponds exactly to the inertial period at the latitude of the array.

The spatial characteristics of the array can be observed from the crosscorrelation function, figure 7, between transponder units 1 and 2 at the ends of the array. Here the uniformity of motion across the array is demonstrated by the high value of the crosscorrelation coefficient at zero lag. The crosscorrelation plot also shows clear evidence of the inertial period in the displacement fluctuations.

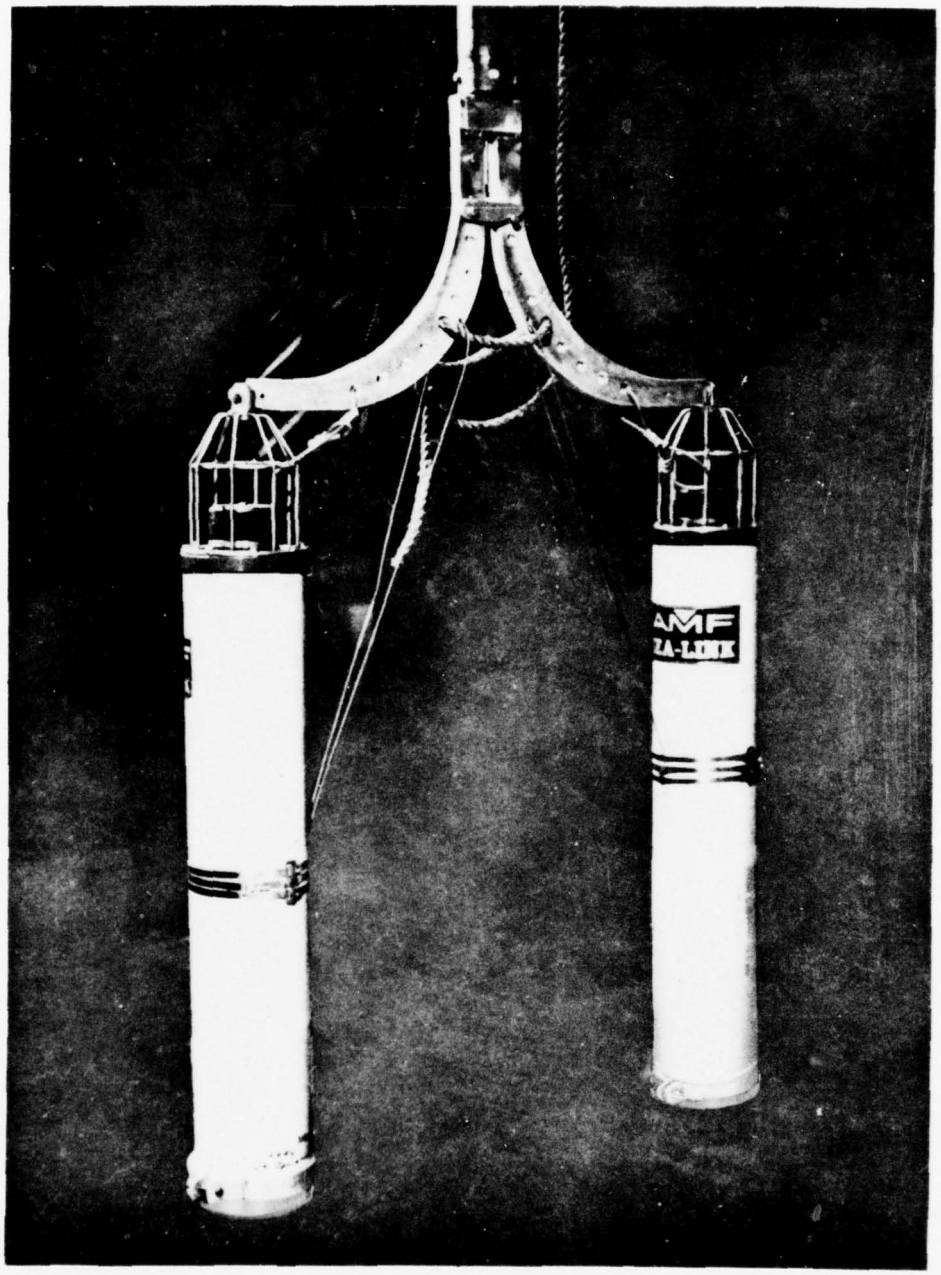

Figure 2. Transponder Assembly

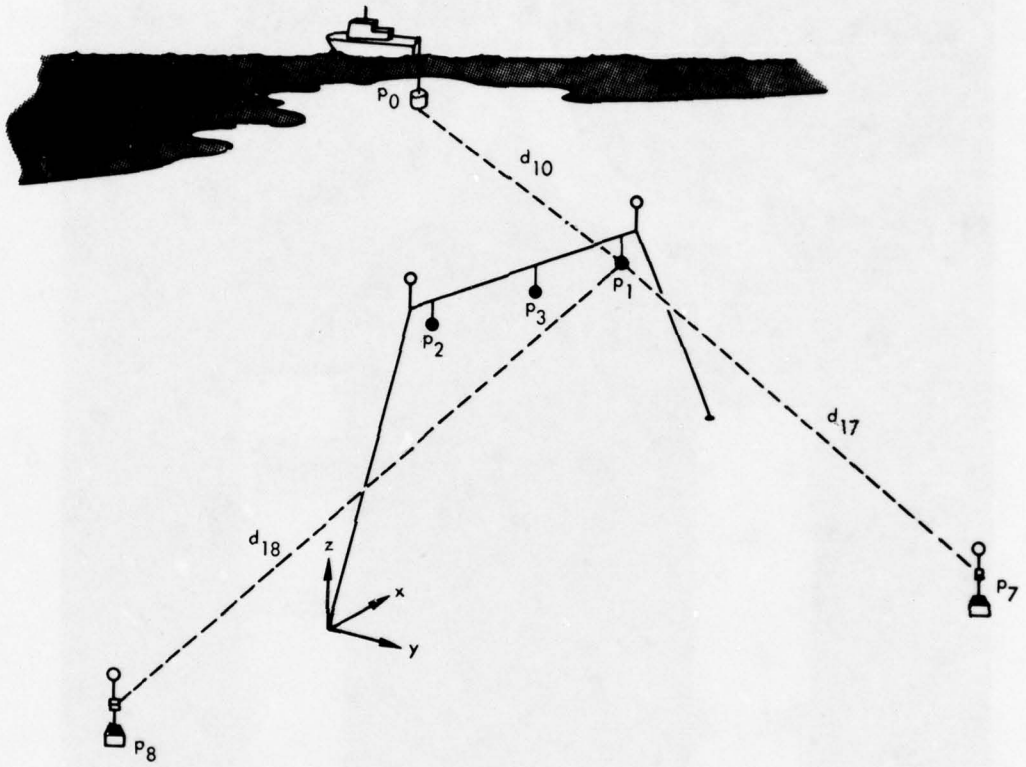

Figure 3. Experimental Configuration

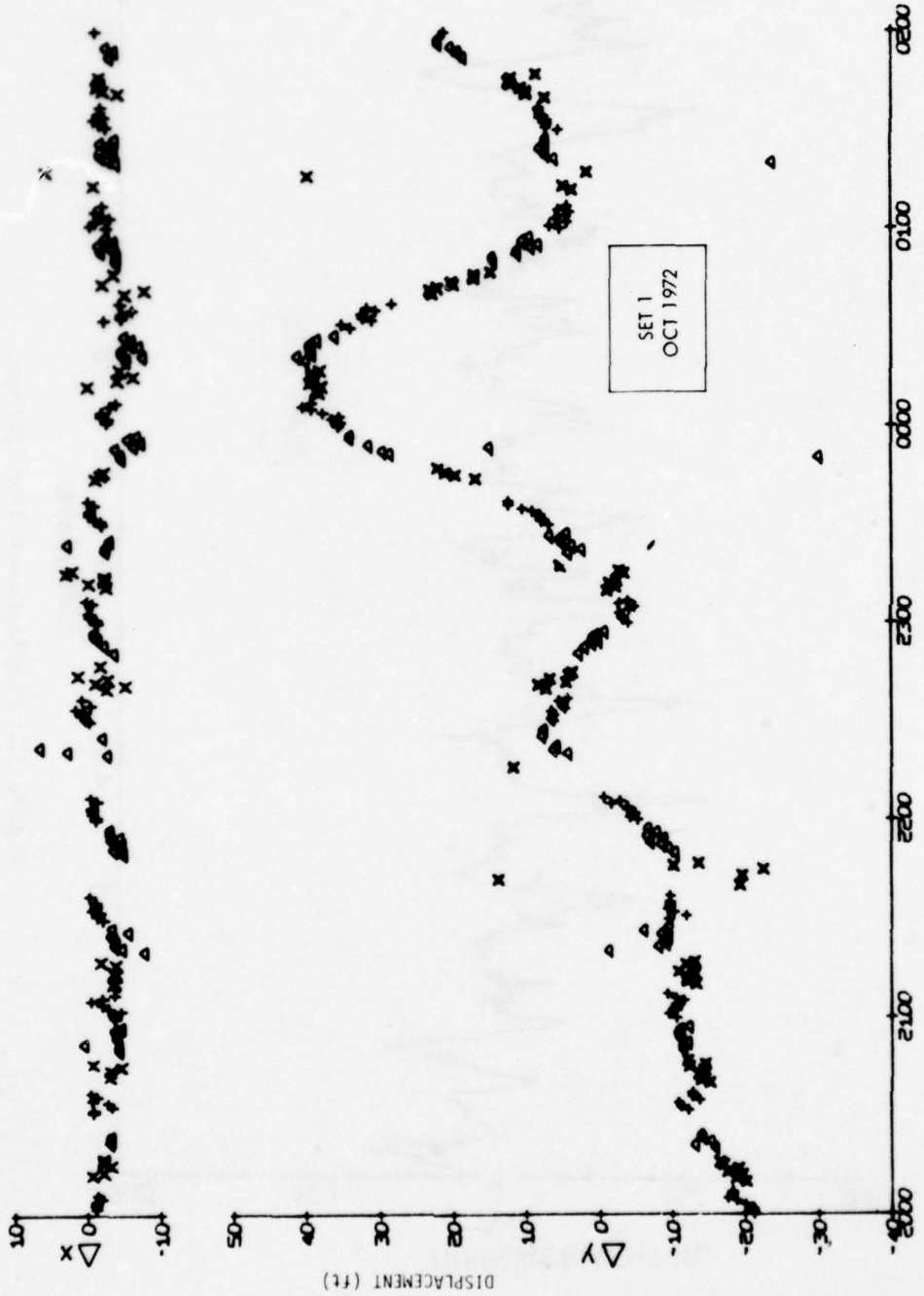

Figure 4. Raw Data

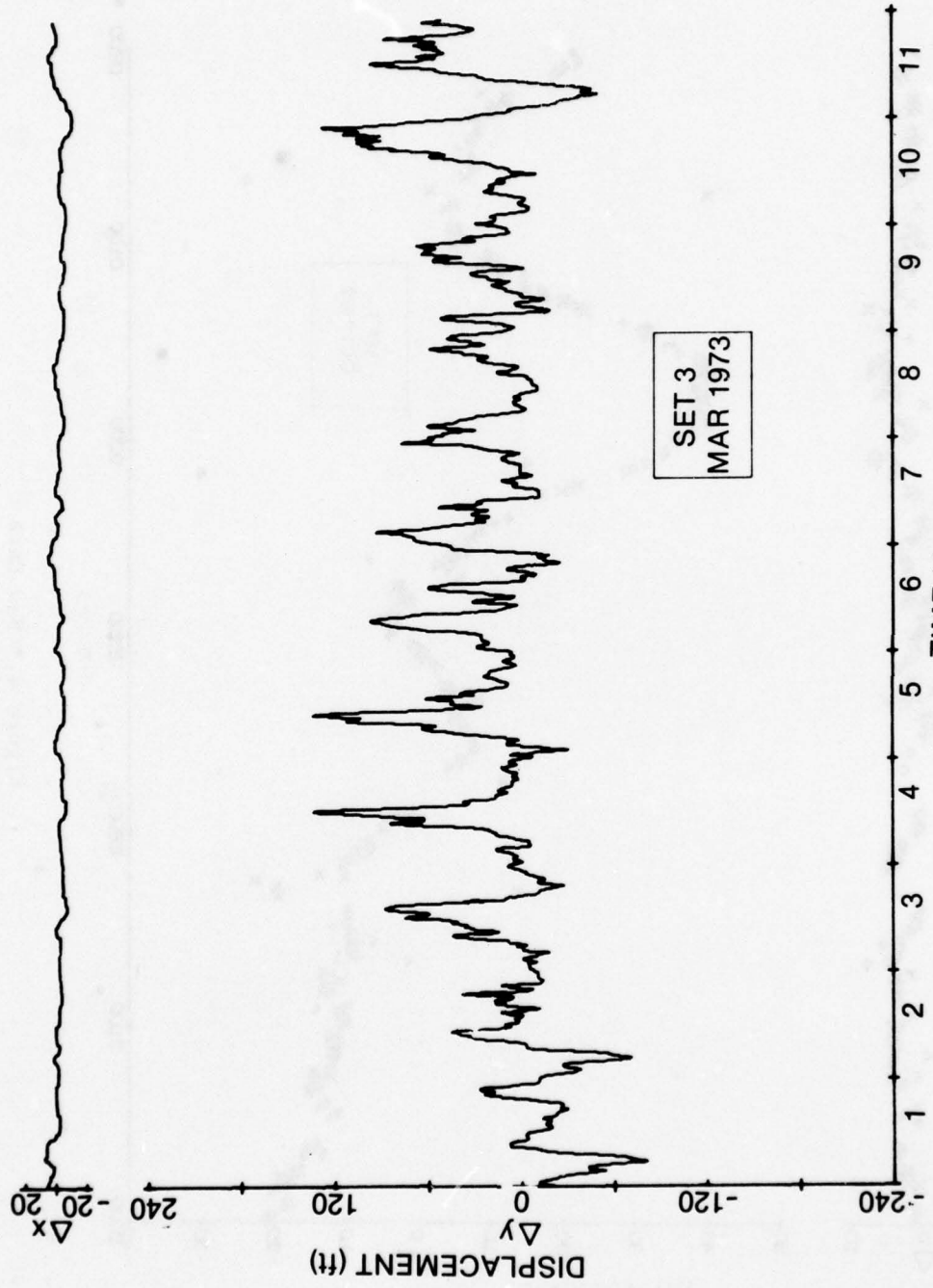

Figure 5. Displacement Time Series

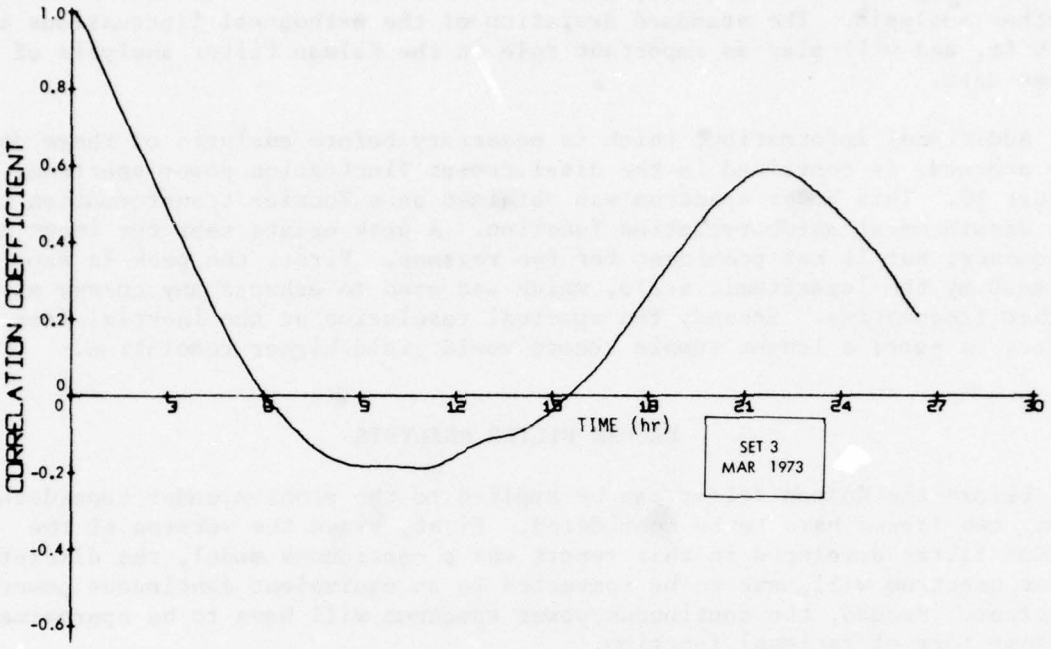

Figure 6. Displacement Autocorrelation Function

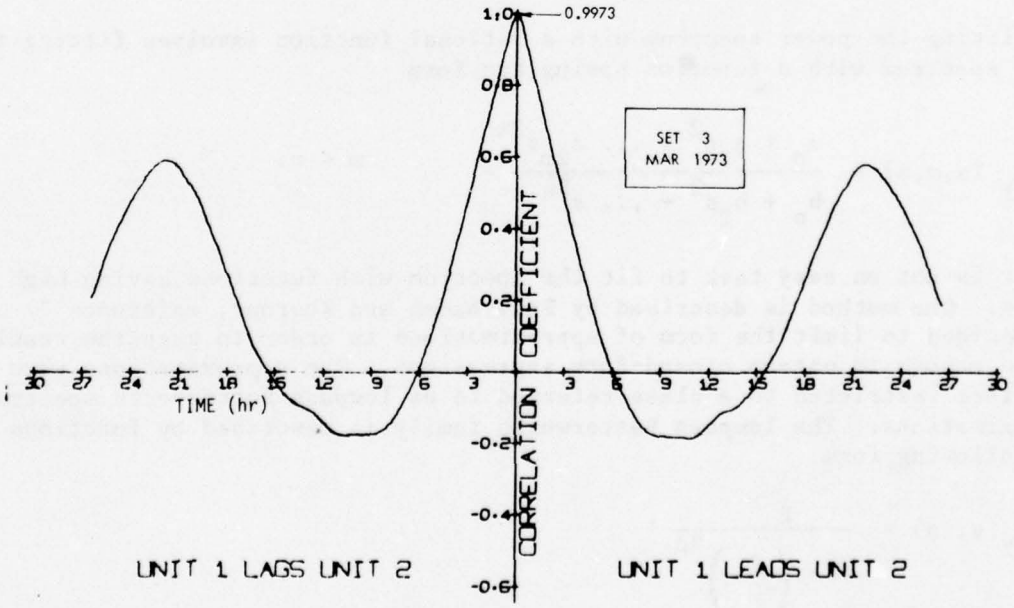

Figure 7. Displacement Crosscorrelation Function

Histograms of the displacements orthogonal to and inline with the array are shown in figures 8 and 9, respectively. The displacements inline with the array are relatively small, and will therefore not be considered in further analysis. The standard deviation of the orthogonal fluctuations is 34.6 ft, and will play an important role in the Kalman filter analysis of these data.

Additional information, which is necessary before analysis of these data can proceed, is contained in the displacement fluctuation power spectrum, figure 10. This power spectrum was obtained as a Fourier transformation of the displacement autocorrelation function. A peak exists near the inertial frequency, but is not prominent for two reasons. First, the peak is suppressed by the logarithmic scale, which was used to enhance any energy at the higher frequencies. Second, the spectral resolution at the inertial frequency is poor; a longer sample record would yield higher resolution.

KALMAN FILTER ANALYSIS

Before the Kalman filter can be applied to the problem under consideration, two issues have to be considered. First, since the version of the Kalman filter developed in this report was a continuous model, the discrete power spectrum will have to be converted to an equivalent continuous power spectrum. Second, the continuous power spectrum will have to be approximated by some form of rational function.

The details of converting the spectrum are shown in appendix A. The initial spectrum is the discrete one-sided spectrum of figure 10. The result of the spectral conversion is shown in figure 11 and represents one half of a two-sided continuous spectrum.

Fitting the power spectrum with a rational function involves fitting the power spectrum with a function having the form

$$R_y(s,m,n) = \frac{a_o + a_2 s^2 + \ldots a_{2m} s^{2m}}{b_o + b_2 s^2 + \ldots s^{2n}} \qquad m < n.$$

It is not an easy task to fit the spectrum with functions having high orders. One method is described by Sanathanan and Koerner, reference 7. It was decided to limit the form of approximations in order to keep the results simple enough to obtain closed-form expressions. The approximations were therefore restricted to a class referred to as lowpass Butterworth spectral approximations. The lowpass Butterworth family is described by functions of the following form

$$R_y(s, n) = \frac{P}{1 - \left(\frac{s}{\omega_c}\right)^{2n}},$$

where n is the number of poles in either half of the s-plane. Only the 1- and 2-pole approximations are considered here, since obtaining closed-form expressions for higher orders is time consuming.

The details of the lowpass Butterworth spectral approximation are covered in appendix B. Briefly, for a given n, the two parameters to estimate are ω_c and P. The two conditions to be satisfied were selected to be:

(1) Total spectral energy = measured data variance,
(2) The frequency approximation error is minimized at the inertial frequency.

Meeting these considerations determines the parameters ω_c and P. The resulting 1- and 2-pole spectral approximations are shown on figure 11, where they are superimposed on the continuous measured spectrum.

All information is now available for the application of the Kalman filter algorithm. The details of these computations are carried out in appendix C (1 pole) and appendix D (2 pole). In both cases (1 and 2 pole), the estimator and the variance of the error of the estimator are determined for the Kalman filter and the Kalman predictor.

In the example under consideration, the noise $\underline{v}(t)$ is very small. Thus, the variance of the error associated with the Kalman filter is nearly zero and almost perfect current estimates of array position can be made. Predicting the position of the array at some time in the future, however, is subject to substantial error. This can be observed in figure 12, where the standard deviation of the error is plotted as a function of time for both predictors. Note that the prediction error starts off near zero for the filtered estimate and approaches the standard deviation of the measured data (34.6 ft) as time increases.

If we arbitrarily define prediction time as

$$\text{Prediction time} = t_p \Rightarrow \left[V_{e_y}(t \mid t_1)\right]^{1/2} \Bigg|_{t = t_p} = \frac{1}{e},$$

the prediction times for the 1-pole and 2-pole predictions are 16 and 109 minutes, respectively. Thus it can be seen that the prediction time is very sensitive to the spectral approximation. The results should not be surprising, however, since the 2-pole spectrum has less high frequency fluctuation than the 1-pole spectrum. Since the slope of the true spectrum lies between the slope of the 1- and 2-pole approximations, it is likely that the true prediction time is bounded by the two prediction time estimates. The true prediction time, however, can be approached only by making higher order approximations to the power spectrum.

SUMMARY AND CONCLUSIONS

The application of the techniques used in this report might seem unnecessarily cumbersome for the treatment of a problem of this nature. However, this example was used only to demonstrate the use of the Kalman method in filtering and predicting stationary time series data. In actual practice, a discrete version of the Kalman filter would probably be used, and numerical results (rather than closed-form expressions) would be desired. Used in this manner, the Kalman filter is simple to implement on a digital computer, and is computationally efficient.

The chief problems in using these methods with stationary time series data are (1) solving the matrix Riccati equation, and (2) fitting the power spectrum with a rational function of high enough order to be a true representation of the real spectrum.

In the particular example used here, the prediction of array position was shown to be highly sensitive to the spectral approximation. Even in the best case considered (2-pole approximation), the prediction time (109 minutes) was relatively short. Higher-order spectral approximations would improve the accuracy or the prediction time estimate but would not increase the prediction time. Thus the possibility of predicting array positions for a long time in the future based on past measurements seems doubtful, unless some deterministic behavior can be established.

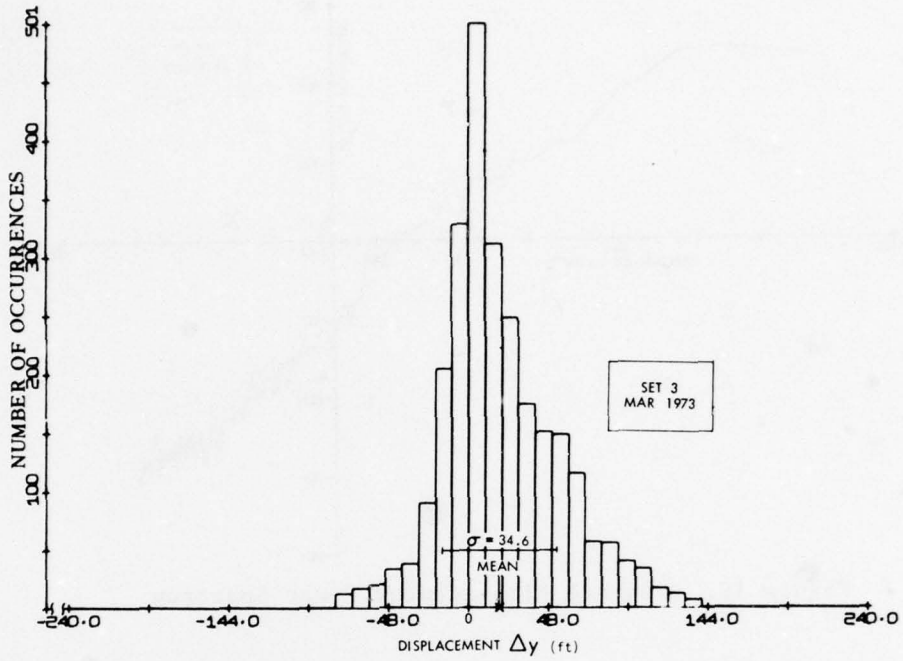

Figure 8. Displacement Histogram (Δy)

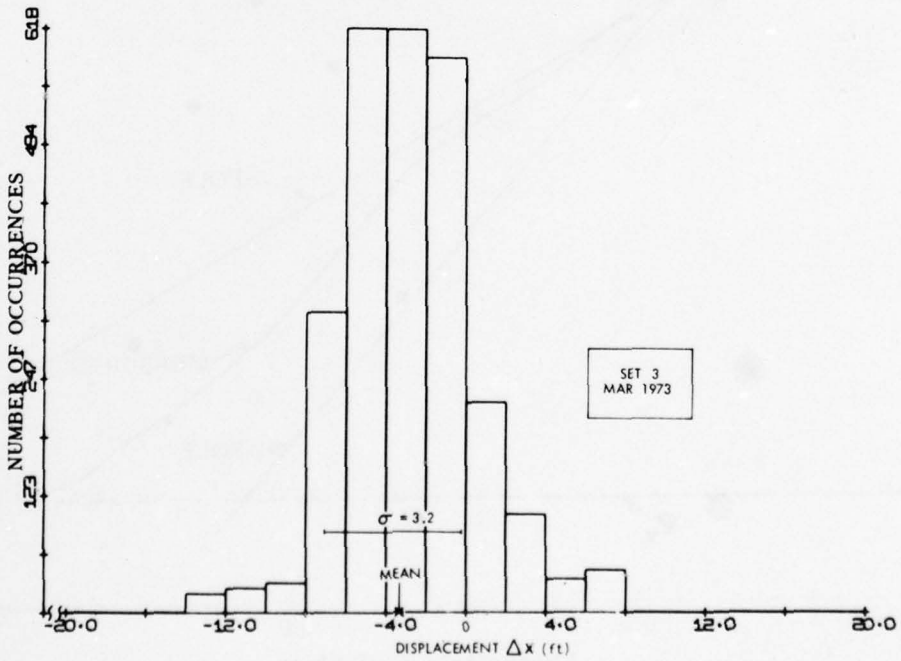

Figure 9. Displacement Histogram (Δx)

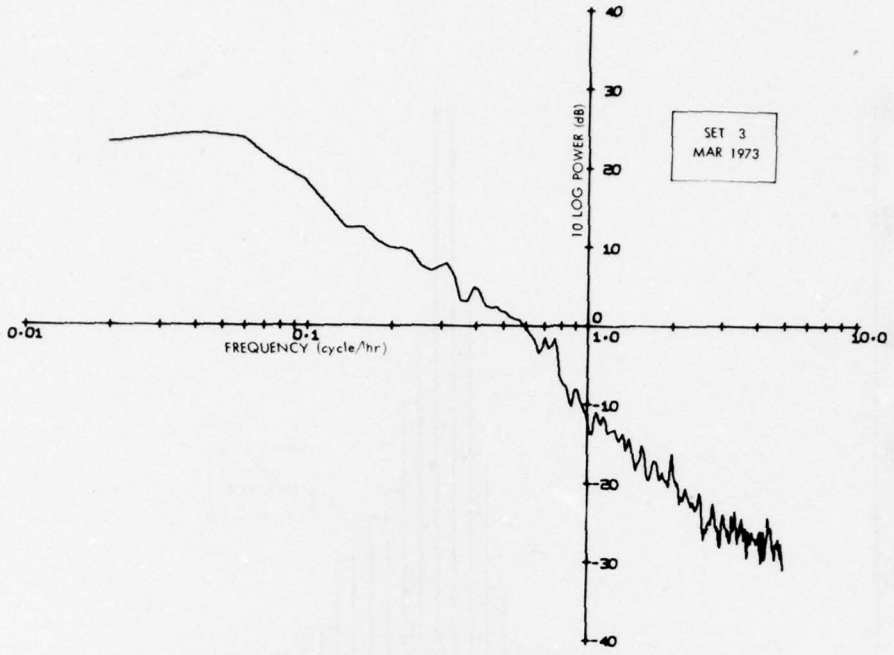

Figure 10. Discrete Displacement Power Spectrum

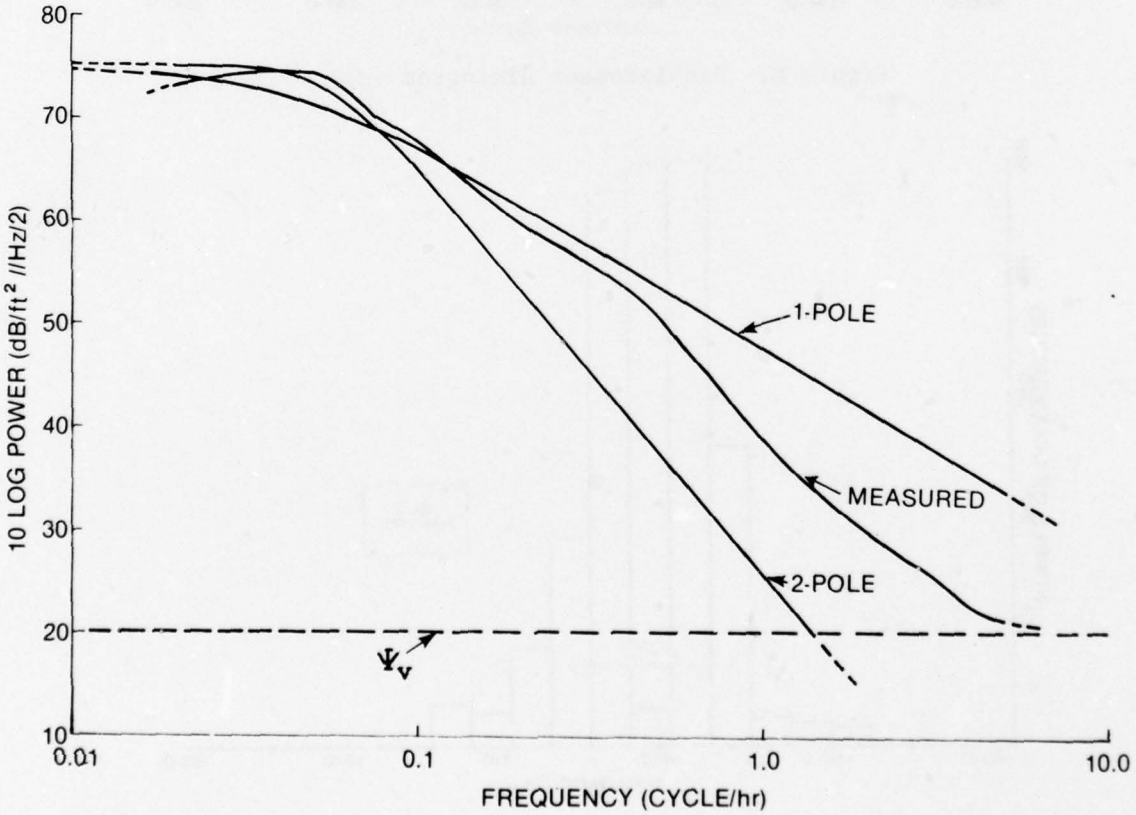

Figure 11. Continuous Displacement Power Spectrum

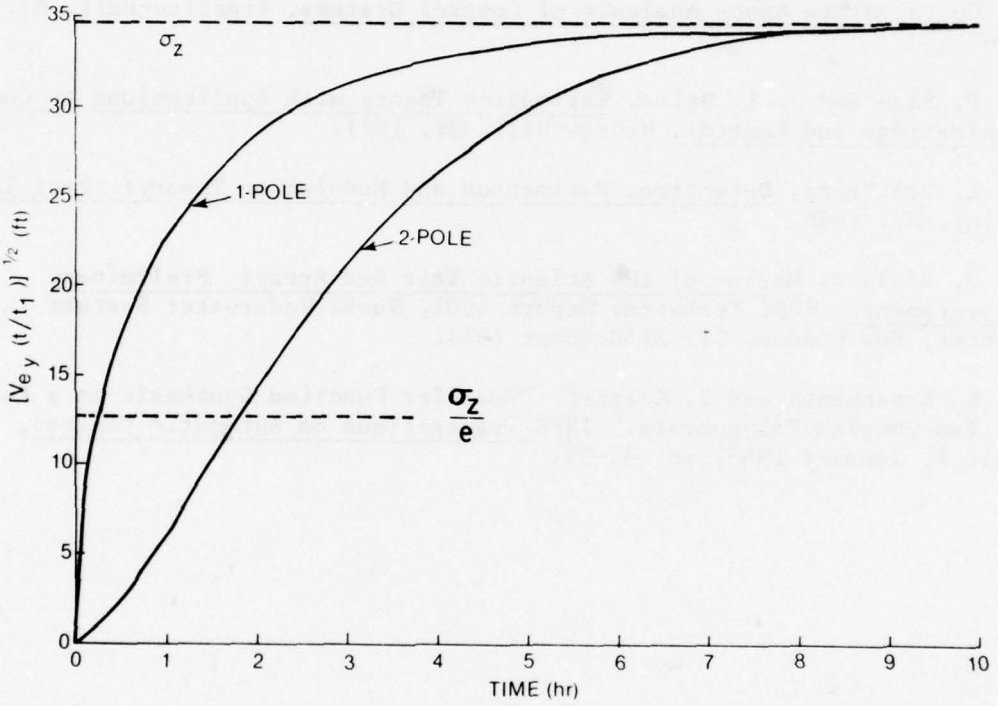

Figure 12. Error Standard Deviation Versus Time

REFERENCES

1. N. Wiener, Extrapolation, Interpolation, and Smoothing of Stationary Time Series, Wiley, NY, 1949.

2. R. E. Kalman, "A New Approach to Linear Filtering and Prediction Problems," Trans. ASME, Part D - Journal of Basic Engineering, vol. 820, March 1960, pp. 34-45.

3. K. Ogata, State Space Analysis of Control Systems, Prentice-Hall, NJ, 1967.

4. A. P. Sage and J. L. Melsa, Estimation Theory with Applications to Communications and Control, McGraw-Hill, NY, 1971.

5. H. L. Van Trees, Detection, Estimation and Modulation Theory: Part I, Wiley, NY, 1968.

6. R. J. Nielsen, Motion of the Atlantic Test Bed Array: Preliminary Measurements, NUSC Technical Report 4601, Naval Underwater Systems Center, New London, CT, 31 October 1973.

7. C. K. Sanathanan and J. Koerner, "Transfer Function Synthesis as a Ratio of Two Complex Polynomials," IEEE Transactions on Automatic Control, vol. 8, January 1963, pp. 56-58.

APPENDIX A

CONVERSION OF THE DISCRETE POWER SPECTRUM TO AN EQUIVALENT CONTINUOUS POWER SPECTRUM

The theory developed in this report is based on a continuous filtering model. Thus it was necessary to convert the discrete power spectrum to a continuous power spectrum in order to apply the results.

The length of the sample was

$$L = 262 \text{ hr.}$$

The sampling rate was

$$f_s = 10 \text{ samples/hr,}$$

which corresponds to a sampling interval of

$$\Delta t = \frac{1}{f_s} = 0.1 \text{ hr.}$$

The total number of samples are

$$N = \frac{L}{\Delta t} = 2620 \text{ samples.}$$

The power spectrum shown in figure 10 was obtained by taking the Fourier transform of the autocorrelation function shown in figure 6. The number of correlation lag values was selected to be

$$m = 0.1\ N,$$

which would make the standard error of the spectral estimates

$$\epsilon = \sqrt{\frac{m}{N}} = \sqrt{0.1}.$$

The length of the two-sided autocorrelation function was then

$$T = \frac{2(0.1\ N)}{\Delta t} = 52.4 \text{ hr.}$$

A discrete Fourier transform of a record of length T results in an equivalent bandwidth of

$$\Delta f = \frac{1}{T} = \frac{1}{52.4} = 0.0191 \text{ cycle/hr.}$$

Each value plotted in figure 10 represents 10 times the log of the one-sided spectral estimate, i.e.,

$$P_k = 10 \log X(k).$$

The sum of all spectral estimates is equal to the variance of the data.

$$\sigma_z^2 = \sum_{k=1}^{262} = X(k) = (34.6)^2$$

with $f_k = k\ \Delta f$.

To convert the one-sided discrete spectrum to a two-sided equivalent continuous spectrum, a bandwidth correction must be made:

$$10 \log [P] = 10 \log \left[\frac{P_k}{2} \left(\frac{1\ (Hz)}{\Delta f\ (Hz)} \right) \right].$$

The continuous spectrum which results is that of figure 11, where the spectral units are $db/ft^2//Hz/2$.

APPENDIX B

LOWPASS BUTTERWORTH SPECTRAL APPROXIMATION

Assume that the power spectrum of the message process can be approximated by a rational function of the form

$$R_y(s,n) = \frac{P}{1-\left(\frac{s}{\omega_c}\right)^{2n}} \text{ or } R_y(\omega,n) = \frac{P}{1+\left(\frac{\omega}{\omega_c}\right)^{2n}}$$

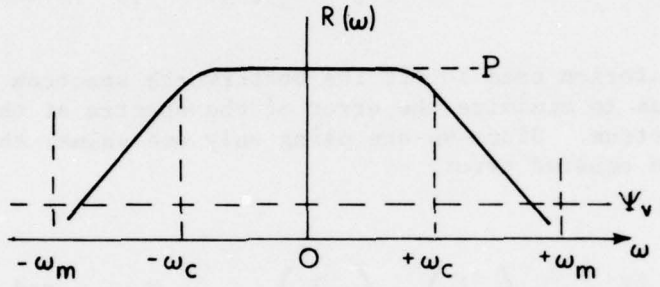

Functions of this type are known as the Butterworth family, where ω_c is the 3 dB down point and n is the number of poles in either half plane of the approximation.

The message spectrum and the measured spectrum are related

where y(t) and v(t) are uncorrelated, and v(t) is assumed to be white noise with

$$\text{cov}\{v(t), v(\tau)\} = \Psi_v \delta(t-\tau).$$

Then for all s or ω,

$$R_z(s) = R_y(s) + \Psi_v \text{ or } R_z(\omega) = R_y(\omega) + \Psi_v.$$

If we integrate both sides over the frequency range for which the measured power spectrum was computed, we have

$$\omega_m = \frac{2\pi f_s}{2} = 2\pi \frac{(10/3600)}{2} = \frac{\pi}{360} \quad \frac{\text{rad}}{\text{s}}$$

$$\int_{-\omega_m}^{+\omega_m} R_z(\omega)d\omega = \sigma_z^2 = \frac{1}{2\pi} \int_{-\omega_m}^{+\omega_m} \frac{P}{1+\left(\frac{\omega}{\omega_c}\right)^{2n}} d\omega + \frac{1}{2\pi} \int_{-\omega_m}^{+\omega_m} \Psi_v \, d\omega \quad .$$

Since $\omega_m >> \omega_c$, we can write

$$\sigma_z^2 \cong \frac{P\omega_c}{2n \sin(\pi/2n)} + \Psi_v \frac{\omega_m}{\pi} .$$

The above expression relates P and ω_c, since all other parameters are known.

The other criterion used to fit the Butterworth spectrum to the measured power spectrum was to minimize the error of the spectra at the peak value of the measured spectrum. Since we are using only one value, this is the same as minimizing the squared error.

Thus with

$$\omega_{peak} = \omega_p = \frac{2\pi}{T_p} = 2\pi \left(\frac{1}{22.5}\right) \left(\frac{1}{3600}\right) = \frac{\pi}{40500} \quad \frac{\text{rad}}{\text{sec}} ,$$

$R_{z_{meas}}(\omega)$ known,

and

$R_{z_{meas}}(\omega_p) = P_{peak} = P_p$, a known constant.

Define

$$\Delta \triangleq R_{z_{meas}}(\omega_p) - R_z(\omega_p)$$

$$\Delta = P_p - \left\{ \frac{P}{1+\left(\frac{\omega_p}{\omega_c}\right)^{2n}} + \Psi_v \right\} ,$$

where

$$P = \left[\sigma_z^2 - \Psi_v \frac{\omega_m}{\pi}\right] \left[2n \sin \frac{\pi}{2n}\right] \frac{1}{\omega_c} .$$

To minimize the error at $\omega = \omega_p$,

$$\frac{d\omega}{d\omega_c} = 0.$$

Solving for ω_c in terms of ω_p results in the following value for ω_c:

$$\omega_c = (2n-1)^{1/2n} \cdot \omega_p.$$

Evaluation of the spectral approximation for the 1- and 2- pole Butterworth spectra results in the following parameter values.

	1 Pole	2 Pole
n	1	2
ω_c(rad/s)	7.76×10^{-5}	1.02×10^{-4}
f_c(cycle/hr)	0.045	0.0584
10 log P ($dB/ft^2//Hz/2$)	74.9	75.2
10 log Ψ_v($dB/ft^2//Hz/2$)	20	20

APPENDIX C

1-POLE COMPUTATIONS

KALMAN 1-POLE FILTER

$\dot{x}(t) = Fx(t) + Gw(t)$ Message model

$z(t) = Hx(t) + v(t)$ Observation model

$y(t) = Hx(t)$

The power spectrum model is

$$R_y(s) = \frac{P}{1-\left(\frac{s}{\omega_c}\right)^2} = \left[R_y(s)\right]^+ \left[R_y(s)\right]^-.$$

The spectral factorization yields

$$R_y(s) = \left[\frac{P^{1/2}\omega_c}{\omega_c + s}\right]^+ \left[\frac{P^{1/2}\omega_c}{\omega_c - s}\right]^- .$$

which results in the following scalar quantities for the matrices:

$$F = -\omega_c \qquad H^T = P^{1/2}\,\omega_c \qquad G = 1$$

$$\text{cov}\,\{w(t),\, w(\tau)\} = \Psi_w\,\delta(t-\tau) = 1\delta(t-\tau)$$

$$\text{cov}\,\{v(t),\, v(\tau)\} = \Psi v\,\delta\,(t-\tau).$$

The filter equation is

$$\dot{\hat{x}}(t) = \left[F-KH\right]\hat{x}(t) + Kz(t) = A\hat{x}(t) + Kz(t),$$

which has a solution given by

$$\hat{x}(t) = \Phi_A(t,-\infty)\,\hat{x}\,(-\infty) + \int_{-\infty}^{t} \Phi_A(t,\,\tau)\,K(\tau)\,z(\tau)\,d\tau,$$

where

$$x\,(-\infty) = 0.$$

The Kalman gain is given by

$$K = V_{e_x}(o)\, H^T \Psi_v^{-1},$$

and the error variance is given by the solution of the matrix Riccati equation

$$0 = FV_{e_x}(o) + V_{e_x}(o)\, F^T - V_{e_x}(o)\, H^T \Psi_v^{-1} HV_{e_x}(o) + G\, \Psi_w\, G^T,$$

where $V_{e_x}(o) = V_{e_x}(t)$ for stationary processes.

Solving the equation, we find

$$V_{e_x}(o) = \frac{\Psi_v}{P\omega_c} \left\{ \left[1 + \frac{P}{\Psi_v} \right]^{1/2} - 1 \right\}$$

and

$$K = \frac{1}{P^{1/2}} \left\{ \left[1 + \frac{P}{\Psi_v} \right]^{1/2} - 1 \right\}.$$

The solution of the transition matrix is given by

$$\Phi_A(t, \tau) = e^{A(t-\tau)} = \alpha_o I = \alpha_o,$$

where

$$\alpha_o = e^{\lambda(t-\tau)},$$

and λ is the eigenvalue of A given by solving

$$| \lambda I - A | = 0,$$

where

$$A = F\text{-}KH = -\omega_c \left[1 + \frac{P}{\Psi_v} \right]^{1/2}.$$

Again by solving the equations, we find that

$$\lambda = -\omega_c \left[1 + \frac{P}{\Psi_v} \right]^{1/2}, \quad \alpha_o = e^{-\omega_c \left[1 + \frac{P}{\Psi_v} \right]^{1/2} (t-\tau)},$$

and the resulting transition matrix is

$$\Phi_A(t, \tau) = e^{-\omega_c \left[1 + \frac{P}{\Psi_v}\right]^{1/2} (t-\tau)} .$$

By substituting the values determined into the solution for the state equation, we find that the state estimate is

$$\hat{x}(t) = \frac{1}{P^{1/2}} \left\{\left[1 + \frac{P}{\Psi_v}\right]^{1/2} - 1\right\} \int_{-\infty}^{t} e^{-\omega_c \left[1 + \frac{P}{\Psi_v}\right]^{1/2} (t-\tau)} z(\tau)\, d\tau.$$

Since

$$\hat{y}(t) = H\, \hat{x}(t) = P^{1/2}\, \omega_c \hat{x}(t),$$

the estimated displacement is

$$\hat{y}(t) = \omega_c \left\{\left[1 + \frac{P}{\Psi_v}\right]^{1/2} - 1\right\} \int_{-\infty}^{t} e^{-\omega_c \left[1 + \frac{P}{\Psi_v}\right]^{1/2} (t-\tau)} z(\tau)\, d\tau.$$

Also, since

$$V_{e_y}(t) = V_{e_y}(o) = H V_{e_x}(o)\, H^T = P\omega_c^2\, V_{e_x}(o),$$

the variance of the error in the estimated position is given by

$$V_{e_y}(t) = V_{e_y}(o) = \omega_c\, \Psi_v \left\{\left[1 + \frac{P}{\Psi_v}\right]^{1/2} - 1\right\}.$$

KALMAN 1-POLE PREDICTION

The predicted displacement is given by

$$\hat{y}(t|t_1) = H\, \hat{x}(t|t_1),$$

where

$$\hat{x}(t|t_1) = \Phi_F(t, t_1)\, \hat{x}(t_1).$$

Since

$$\hat{x}(t) = \hat{y}(t)/P^{1/2}\omega_c,$$

we can write the predictor equation as

$$\hat{y}(t|t_1) = \hat{y}(t_1)\, \Phi_F(t, t_1).$$

The solution of the transition matrix is given by

$$\Phi_F(t, t_1) = e^{F(t-t_1)} = \alpha_o I = \alpha_o,$$

where

$$\alpha_o = e^{\lambda(t-t_1)}$$

and λ is the eigenvalue of F given by solving

$$|\lambda I - F| = 0$$

Solving the equations, we find

$$\lambda = F = \omega_c, \quad \alpha_o = e^{-\omega_c (t-t_1)},$$

and the resulting transition matrix is

$$\Phi_F(t, t_1) = e^{-\omega_c(t-t_1)}.$$

Substituting into the predictor equation, we find the predicted displacement is given by

$$\hat{y}(t|t_1) = \hat{y}(t_1)\, e^{-\omega_c(t-t_1)} \qquad \text{for } t \geq t_1.$$

The variance of the error of the predicted estimate is given by solving

$$V_{e_y}(t|t_1) = H V_{e_x}(t|t_1)\, H^T,$$

where

$$V_{e_x}(t|t_1) = \Phi_F(t, t_1)\, V_{e_x}(t_1)\, \Phi_F^T(t, t_1)$$

$$+ \int_{t_1}^{t} \Phi_F(t, \tau)\, G(\tau)\, \Psi_w(\tau)\, G^T(\tau)\, \Phi^T(t, \tau)\, d\tau.$$

In the problem under consideration, this reduces to

$$V_{e_x}(t|t_1) = V_{e_x}(t_1)\, e^{-2\omega_c(t-t_1)} + \frac{1}{2\omega_c}\left[1 - e^{-2\omega_c(t-t_1)}\right],$$

and the resulting variance of the error in the predicted displacement is given by

$$V_{e_y}(t|t_1) = V_{e_y}(t_1)\, e^{-2\omega_c (t-t_1)} + \frac{P\omega_c}{2}\left[1 - e^{-2\omega_c (t-t_1)}\right]$$

for $t \geq t_1$.

APPENDIX D

2-POLE COMPUTATIONS

KALMAN 2-POLE FILTER

$$\dot{\underline{x}}(t) = F\underline{x}(t) + G\underline{w}(t) \qquad \text{Message model}$$

$$z(t) = H\underline{x}(t) + v(t) \qquad \text{Observation model}$$

$$y(t) = H\underline{x}(t)$$

The power spectrum model is

$$R_y(s) = \frac{P}{1 - \left(\frac{s}{\omega_c}\right)^4} = \left[R_y(s)\right]^+ \left[R_y(s)\right]^- ,$$

the spectral factorization yields

$$R_y(s) = \left[\frac{P^{1/2}\omega_c^2}{\omega_c^2 + \sqrt{2}\,\omega_c s + s^2}\right]^+ \left[\frac{P^{1/2}\omega_c^2}{\omega_c^2 - \sqrt{2}\,\omega_c s + s}\right]^- ,$$

which results in the following matrices

$$F = \begin{bmatrix} 0 & 1 \\ -\omega_c^2 & -\sqrt{2}\omega_c \end{bmatrix} \quad H^T = \begin{bmatrix} P^{1/2}\omega_c^2 \\ 0 \end{bmatrix} \quad G = I$$

$$\text{cov}\ \{\underline{w}(t), \underline{w}(\tau)\} = \Psi_{\underline{w}}\,\delta(t-\tau) = \begin{bmatrix} 0 & 0 \\ 0 & 1 \end{bmatrix}\delta(t-\tau)$$

$$\text{cov}\ \{v(t), v(\tau)\} = \Psi_v\,\delta(t-\tau).$$

The filter equation is

$$\dot{\hat{\underline{x}}}(t) = \left[F - KH\right]\hat{\underline{x}}(t) + Kz(t) = A\hat{\underline{x}}(t) + Kz(t),$$

which has a solution given by

$$\hat{\underline{x}}(t) = \Phi_A(t, -\infty)\,\hat{\underline{x}}(-\infty) + \int_{-\infty}^{t} \Phi_A(t, \tau)\,K(\tau)\,z(\tau)\,d\tau ,$$

where

$$\hat{\underline{x}}(-\infty) = \underline{0}.$$

The Kalman gain is given by

$$K = V_{e_{\underline{x}}}(o)\, H^T \Psi_v^{-1} H V_{e_{\underline{x}}}(o) ,$$

and the error variance is given by the solution of the matrix Riccati equation

$$0 = F V_{e_{\underline{x}}}(o) + V_{e_{\underline{x}}}(o)\, F^T - V_{e_{\underline{x}}}(o)\, H^T \Psi_v^{-1} H V_{e_{\underline{x}}}(o) + G \Psi_{\underline{w}}\, G^T,$$

where $V_{e_{\underline{x}}}(t) = V_{e_{\underline{x}}}(o)$ for stationary processes.

Define

$$S \triangleq \left\{ \left[1 + \frac{p}{\Psi_v} \right]^{1/4} - 1 \right\} .$$

Solving the equations, we find

$$V_{e_{\underline{x}}}(o) = \begin{bmatrix} \dfrac{\sqrt{2}\Psi_v}{p\omega_c^3}\, S & \dfrac{\Psi_v}{p\omega_c^2}\, S^2 \\ \dfrac{\Psi}{p\omega_c^2}\, S^2 & \dfrac{\sqrt{2}\Psi_v}{p\omega_c}\, S\,(1 + S + S^2) \end{bmatrix}$$

and

$$K = \begin{bmatrix} \dfrac{\sqrt{2}}{p^{1/2}\omega_c}\, S \\ \dfrac{1}{p^{1/2}}\, S^2 \end{bmatrix} .$$

The solution of the transition matrix is given by

$$\Phi_A(t, \tau) = e^{A(t-\tau)} = \alpha_0 I + \alpha_1 A$$

when the α_i are the solution of the set of equations

$$\alpha_0 + \alpha_1 \lambda_1 = e^{\lambda_1 (t-\tau)}$$

$$\alpha_0 + \alpha_1 \lambda_2 = e^{\lambda_2(t-\tau)},$$

and the λ_i are the eigenvalues of A which we obtain by solving

$$|\lambda I - A| = 0,$$

where

$$A = F - KH = \begin{bmatrix} \sqrt{2}\omega_c S & \\ -\omega_c^2 & -\omega_c^2 S^2 \quad -\frac{1}{\sqrt{2}\omega_c} \end{bmatrix}.$$

Solving the equations, we find

$$\lambda_1 = \frac{-\sqrt{2}\omega_c (1 + S)}{2} (1 + j) \text{ and } \lambda_2 = \frac{-\sqrt{2}\omega_c (1 + S)}{2} (1 - j),$$

also

$$\alpha_0 = e^{\frac{-\omega_c (1 + S) (t - \tau)}{\sqrt{2}}} \left\{ \cos\left[\frac{\omega_c (1 + S) (t - \tau)}{\sqrt{2}}\right] + \sin\left[\frac{\omega_c (1 + S) (t - \tau)}{\sqrt{2}}\right] \right\}$$

$$\alpha_1 = \frac{\sqrt{2}}{\omega_c (1 + S)} \; e^{\frac{-\omega_c (1 + S) (t - \tau)}{\sqrt{2}}} \sin\left[\frac{\omega_c (1 + S) (t - \tau)}{\sqrt{2}}\right]$$

and the resulting transition matrix is

$$\Phi_A(t, \tau) = \begin{bmatrix} \Phi_{A_{11}}(t, \tau) & \Phi_{A_{12}}(t, \tau) \\ \Phi_{A_{21}}(t, \tau) & \Phi_{A_{22}}(t, \tau) \end{bmatrix},$$

where

$$\Phi_{A_{11}}(t, \tau) = e^{\frac{-\omega_c (1 + S) (t - \tau)}{2}} \left\{ \cos\left[\frac{\omega_c (1 + S) (t - \tau)}{\sqrt{2}}\right] + \left(\frac{1 - S}{1 + S}\right) \sin\left[\frac{\omega_c (1 + S) (t - \tau)}{\sqrt{2}}\right] \right\}$$

$$\phi_{A_{12}}(t, \tau) = \frac{\sqrt{2}}{\omega_c(1 + S)} \; e^{\frac{-\omega_c (1 + S)(t - \tau)}{\sqrt{2}}} \sin\left[\frac{\omega_c (1 + S)(t - \tau)}{\sqrt{2}}\right]$$

$$\Phi_{A_{21}}(t, \tau) = \frac{-\sqrt{2}\omega_c (1 + S^2)}{1 + S} \; e^{\frac{-\omega_c (1 + S)(t - \tau)}{\sqrt{2}}} \sin\left[\frac{\omega_c (1 + S)(t - \tau)}{\sqrt{2}}\right]$$

$$\Phi_{A_{22}}(t, \tau) = e^{\frac{-\omega_c (1 + S)(t - \tau)}{\sqrt{2}}} \left\{\cos\left[\frac{\omega_c (1 + S)(t - \tau)}{\sqrt{2}}\right] + \left(\frac{S - 1}{S + 1}\right) \sin\left[\frac{\omega_c (1 + S)(t - \tau)}{\sqrt{2}}\right]\right\}$$

Substituting the values determined into the solution for the state equation, we find that the state estimate is

$$\underline{x}(t) = \int_{-\infty}^{t} \begin{bmatrix} \frac{\sqrt{2}\, S}{p^{1/2}\omega_c} \; e^{\frac{-\omega_c (1 + S)(t - \tau)}{\sqrt{2}}} \left\{\cos\left[\frac{\omega_c (1 + S)(t - \tau)}{\sqrt{2}}\right] + \sin\left[\frac{\omega_c (1 + S)(t - \tau)}{\sqrt{2}}\right]\right\} \\ \\ \frac{S}{p^{1/2}} \; e^{\frac{-\omega_c (1 + S)(t - \tau)}{\sqrt{2}}} \left\{S \cos\left[\frac{\omega_c (1 + S)(t - \tau)}{\sqrt{2}}\right] + (2 - S) \sin\left[\frac{\omega_c (1 + S)(t - \tau)}{\sqrt{2}}\right]\right\} \end{bmatrix} z(\tau)\, d\tau.$$

Since $\hat{y}(t) = H\hat{\underline{x}}(t) = p^{1/2}\, \omega_c^2\, \hat{x}_1(t)$,

the estimated displacement is

$$\hat{y}(t) = \sqrt{2}\,\omega_c\, S \int_{-\infty}^{t} e^{\frac{-\omega_c (1+S)(t-\tau)}{\sqrt{2}}} \left\{ \cos\left[\frac{\omega_c (1+S)(t-\tau)}{\sqrt{2}}\right] + \sin\left[\frac{\omega_c (1+S)(t-\tau)}{\sqrt{2}}\right] \right\} z(\tau)\,d\tau$$

$$S \triangleq \left\{ \left[1 + \frac{P}{\Psi_v} \right]^{1/4} - 1 \right\} .$$

Also, since

$$V_{e_y}(t) = V_{e_y}(o) = H V_{e_{\underline{x}}}(o)\, H^T = P\omega_c^4\, V_{e_{x_{11}}}(o) \quad ,$$

the variance of the error in the estimated position is given by

$$V_{e_y}(t) = V_{e_y}(o) = \sqrt{2}\,\omega_c\,\Psi_v \left\{ \left[1 + \frac{P}{\Psi_v} \right]^{1/4} - 1 \right\} .$$

KALMAN 2-POLE PREDICTION

The predicted displacement is given by

$$\hat{y}(t|t_1) = H\,\hat{\underline{x}}\,(t|t_1),$$

where

$$\hat{\underline{x}}\,(t|t_1) = \Phi_F\,(t, t_1)\,\hat{\underline{x}}\,(t_1).$$

Since

$$\hat{\underline{x}}\,(t) = \begin{bmatrix} \hat{x}_1(t) \\ \hat{x}_2(t) \end{bmatrix} = \begin{bmatrix} \hat{y}(t)/\,P^{1/2}\omega_c^2 \\ \dot{\hat{y}}(t)/\,P^{1/2}\omega_c^2 \end{bmatrix} ,$$

we can write the predictor equation as

$$\hat{y}(t|t_1) = \hat{y}(t_1)\,\Phi_{11}(t, t_1) + \dot{\hat{y}}(t_1)\,\Phi_{12}(t, t_1).$$

The solution of the transition matrix is given by

$$\Phi_F(t, t_1) = e^{F(t-t_1)} = \alpha_0 I + \alpha_1 F,$$

where the α_i are the solution of the set of equations

$$\alpha_0 + \alpha_1\lambda_1 = e^{\lambda_1(t-t_1)}$$

$$\alpha_0 + \alpha_1\lambda_2 = e^{\lambda_2(t-t_1)},$$

and the λ_i are the eigenvalues of F which are obtained by solving

$$| \lambda I - F | = 0.$$

Solving the equations, we find that

$$\lambda_1 = \frac{-\omega_c}{\sqrt{2}} [1 + j] \text{ and } \lambda_2 = \frac{-\omega_c}{\sqrt{2}} [1 - j] ;$$

also,

$$\alpha_0 = e^{\frac{-\omega_c}{\sqrt{2}}(t-t_1)} \left\{\sin \frac{\omega_c}{\sqrt{2}} (t-t_1) + \cos \frac{\omega_c}{\sqrt{2}} (t-t_1)\right\}$$

$$\alpha_1 = \frac{\sqrt{2}}{\omega_c} e^{\frac{-\omega c}{\sqrt{2}}(t-t_1)} \left\{\sin \frac{\omega_c}{\sqrt{2}} (t-t_1)\right\},$$

and the resulting transition matrix is

$$\Phi_F(t,t_1) = \left[\begin{array}{c|c} e^{\frac{-\omega_c}{\sqrt{2}}(t-t_1)} \left\{\sin \frac{\omega_c}{\sqrt{2}}(t-t_1) + \cos \frac{\omega_c}{\sqrt{2}} (t-t_1)\right\} & \frac{\sqrt{2}}{\omega_c} e^{\frac{-\omega_c}{\sqrt{2}}(t-t_1)} \left\{\sin \frac{\omega_c}{\sqrt{2}}(t-t_1)\right\} \\ \hline -\sqrt{2}\omega_c e^{\frac{-\omega_c}{\sqrt{2}}(t-t_1)} \left\{\sin \frac{\omega_c}{\sqrt{2}}(t-t_1)\right\} & e^{\frac{-\omega_c}{\sqrt{2}}(t-t_1)} \left\{\cos \frac{\omega_c}{\sqrt{2}} (t-t_1) - \sin \frac{\omega_c}{\sqrt{2}} (t-t_1)\right\} \end{array}\right]$$

Substituting into the predictor equation, we find the predicted value is given by

$$\hat{y}(t|t_1) = e^{\frac{-\omega_c}{\sqrt{2}}(t-t_1)}\left\{\left[\cos\frac{\omega_c}{\sqrt{2}}(t-t_1) + \sin\frac{\omega_c}{\sqrt{2}}(t-t_1)\right]\hat{y}\right.$$

$$\left.+\left[\frac{\sqrt{2}}{\omega_c}\sin\frac{\omega_c}{\sqrt{2}}(t-t_1)\right]\dot{\hat{y}}\right\} \quad \text{for } t \geq t_1.$$

The variance of the error of the predicted estimate is given by solving

$$V_{e_y}(t|t_1) = HV_{e_{\underline{x}}}(t|t_1)\,H^T,$$

where

$$V_{e_{\underline{x}}}(t|t_1) = \Phi_F(t, t_1)\,V_{e_{\underline{x}}}(t_1)\,\Phi_F^T(t, t_1)$$

$$+ \int_{t_1}^{t} \Phi_F(t, \tau)\,G(\tau)\,\Psi_{\underline{w}}(\tau)\,G^T(\tau)\,\Phi^T(t, \tau)\,d\tau.$$

In the problem under consideration, these equations simplify to

$$V_{e_y}(t|t_1) = p\omega_c^4\; V_{e_{x_{11}}}(t|t_1)$$

and

$$V_{e_{x_{11}}}(t|t_1) = \Phi_{F_{11}}(t, t_1)\left[V_{e_{x_{11}}}(t_1)\,\Phi_{F_{11}}(t, t_1) + V_{e_{x_{12}}}(t_1)\,\Phi_{F_{12}}(t, t_1)\right]$$

$$+ \Phi_{F_{12}}(t, t_1)\left[V_{e_{x_{21}}}(t_1)\,\Phi_{F_{11}}(t, t_1) + V_{e_{x_{22}}}(t_1)\,\Phi_{F_{12}}(t, t_1)\right]$$

$$+ \int_{t_1}^{t} \Phi_{F_{12}}^2(t, \tau)\,d\tau.$$

Substituting the values previously determined for these expressions, we have

$$V_{e_y}(t|t_1) = V_{e_y}(t_1)\, e^{-\sqrt{2}\omega_c(t-t_1)}\left\{1 + \left\{1 + \left\{\left[1 + \frac{p}{\Psi_v}\right]^{1/4} - 1\right\}\right\}\right.$$

$$\left\{2 \sin \frac{\omega_c}{\sqrt{2}}(t-t_1) \cos \frac{\omega_c}{\sqrt{2}}(t-t_1)\right\}$$

$$+ \left\{\left\{\left[1 + \frac{p}{\Psi_v}\right]^{1/4} - 1\right\}^2 - 1\right\} 2 \sin^2 \frac{\omega_c}{\sqrt{2}}(t-t_1)\Bigg\}$$

$$+ \frac{p\omega_c}{2\sqrt{2}} \left\{1 + e^{-\sqrt{2}\omega_c(t-t_1)}\left[2 \sin^2 \frac{\omega_c}{\sqrt{2}}(t-t_1)\right.\right.$$

$$\left.\left. + 2 \sin \frac{\omega_c}{\sqrt{2}}(t-t_1) \cos \frac{\omega_c}{\sqrt{2}}(t-t_1) + 1\right]\right\} \quad \text{for } t \geq t_1.$$

INITIAL DISTRIBUTION LIST

Addressee	No. of Copies
ASN(R&D)	1
ONR, ONR-102-OS, -220, -102, -480, -481, -485	7
CNO, OP-02, -095, -098, -951, -955, -96, -981H1(CDR J. Dooley), OP-955F1	9
CNM, MAT-08T21, ASW-122, -111, -24, NMAT-03L(J. Probus)	5
DDR&E (Dr. D. Hyde, R. Moore)(2), (G. Cann)	3
NAV SURFACE WEAPONS CENTER, WHITE OAK LABORATORY	1
NRL, (Dr. B. Adams, A. Gotthardt, R. Rojas, Dr. R. Heitmeyer)	5
NORDA	1
OCEANAV	1
NAVOCEANO, Code 241, 240	3
NAVELECSYSCOM, ELEX 03, PME-124 (CAPT Cox), ELEX 320 (CDR A. Miller)	3
NAVFACENGCOM	1
NAVSEASYSCOM, SEA-03C, -032, -06H1-1, -06H2, -09G32(4)	8
NAVAIRDEVCEN	1
DTNSRDC	1
NAVCOASTSYSLAB	1
NAVSURFWPNCEN	1
NAVOCEANSYSCEN, Code 6565	2
NAVSEC, SEC-6000, -6034	2
CHESNAVFACENGCOM (FPO-IP3)	1
NAVPGSCOL	1
DDC, ALEXANDRIA	12
NATIONAL RESEARCH COUNCIL (COMMITTEE UNDERSEA WARFARE)	1
WEAPON SYSTEM EVALUATION GROUP	1
WOODS HOLE OCEANOGRAPHIC INSTITUTION	1
ARPA, Program Office, R. Gustafson, R. Cook, CDR V. Simmons, Research Center (T. Kooij)	5
Atlas (A. C. Hill) (Atlas Contract No. N00140-78-C-6239)	1
BBN (J. Heine) (BBN Contract No. N00140-75-C-0532)	1
Bendix Electrodynamics (J. Bradbury)(Bendix Contract No. N00140-76-C-6538)	1
CEL (Dr. W. Nordell, 44)	1
Celmark Engineering (J. Schaefer)(Celmark Contract N00140-78-C-6544)	1
Emerson & Cuming, Inc. (L. Watkins) (Emerson & Cuming Contract N00140-78-C-6214)	1
MAR, Inc. (C. Veitch) (MAR Contract No. N00140-78-D-6054)	1
MAR, Inc. (J. Franklin) (MAR Contract No. N00140-78-D-6054)	1
Norfolk Naval Shipyard, St. Juliens Creek Annex (LCDR Fox, LTJG R. Walling)	1
Norfolk Naval Shipyard (Mr. O'Brien, 140)	1
NOSC (Dr. R. Smith, G. Wilkins)	2
OPTEVFOR (LCDR J. Tolbert, 421)	1
ORI (J. Bowen), NAVELEC/ORI Contract No. N0039-76-C-0327)	1
Raytheon Submarine Signal Division (R. Howland) (Raytheon Contract No. N00140-76-C-6110)	1
Samson Ocean Systems (R. Hildebrand)(Samson Contract N00140-78-C-6391)	1

INITIAL DISTRIBUTION LIST (Cont'd)

Addressee	No. of Copies
SSPO (Lt. W. Watkins)	1
CO. USS SPIEGEL GROVE (LSD-32)	2
Teledyne Exploration (C. Berglund) (Teledyne Contract No. N66604-77-M-2652)	1
Unidyne Corp. (J. Smith)(Unidyne Contract No. N00140-77-D-6043)	1